Journal of Medicinal Chemistry

Brief Article

pubs.acs.org/jmc

Identification of Antitubercular Benzothiazinone Compounds by Ligand-Based Design

Tomislav Karoli,[†] Bernd Becker,[†] Johannes Zuegg,[†] Ute Möllmann,[‡] Soumya Ramu,[†] Johnny X. Huang,[†] and Matthew A. Cooper*[,†]

[†]Institute for Molecular Bioscience, University of Queensland, St. Lucia, Queensland 4072, Australia

[‡]Department of Molecular and Applied Microbiology, Leibniz Institute for Natural Product Research and Infection Biology, Hans Knoell Institute, Beutenbergstrasse 11a, D-07745 Jena, Germany

Supporting Information

ABSTRACT: 1,3-Benzothiazin-4-ones (BTZs) are a novel class of TB drug candidates with potent activity against *M. tuberculosis*. An in silico ligand-based model based on structure−activity data from 170 BTZ compounds was used to design a new series. Compounds were tested against a panel of mycobacterial strains and were profiled for cytotoxicity, stability, and antiproliferative effects. Several of the compounds showed improved activity against MDR-TB while retaining low toxicity with higher microsomal, metabolic, and plasma stability.

INTRODUCTION

Tuberculosis (TB), an infectious disease most commonly caused by *Mycobacterium tuberculosis* (*Mtb*), claims ∼2 million lives each year. According to the most recent WHO report, 4.7 million cases of TB were recorded in 2009, 250 000 of which were estimated to involve multidrug resistant TB (MDR-TB). Of these MDR-TB cases, around 7% (up to 33% in some countries) have been shown to be extensively drug resistant (XDR-TB).[1] The increasing failure of the current therapies for TB and the dire lack of drugs in the development pipeline highlight the urgent need to develop new drugs.[2]

1,3-Benzothiazin-4-ones (BTZs, Figure 1) are a novel class of TB drug candidates with potent activity against *Mtb* in vitro and in vivo.[3] Previous studies[3,4] identified the racemic benzothiazinone **1** (BTZ-10526038) and its chiral analogue **2** (BTZ-10526043, BTZ043) (Figure 1) as lead structures. Compound **2** exhibits a minimum inhibitory concentration (MIC) of 1 ng/mL against *Mtb* H37Rv, a factor of 20 below that of the frontline TB drug isoniazid (INH). The target of **2** is decaprenylphosphoryl-β-D-ribose 2′-epimerase (DprE1, Rv3790), which with DprE2 (Rv3791) is critical for the synthesis of cell-wall arabinans and catalyzes the epimerization of decaprenylphosphoryl-β-D-ribose to decaprenylphosphoryl-β-D-arabinose.[5] It has been shown[6] that BTZ compounds act as suicide inhibitors after enzymatic activation of the nitro as the nitroso and subsequent covalent reaction with Cys387 of DprE1resulting in enzymatic inhibition.

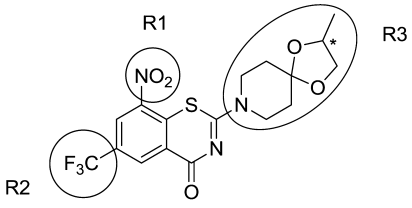

(*RS*) 1 (BTZ-10526038)
(*S*) 2 (BTZ-10526043)

Figure 1. Lead benzothiazinone structures. R1 acts as site of covalent addition to DprE1 after enzymatic activation, and an electron withdrawing group at R2 is required. Variation is permitted in R3. Both enantiomers (chiral center highlighted by ∗) are equipotent in vitro.

A review of the available pharmacokinetics of these BTZ compounds revealed that many had poor solubility and that the bioavailability and ADME/T properties could be improved. Therefore, the principle goal of this study was to design a second generation series with increased solubility and to explore the metabolic stability and toxicity profile of the new compounds.

METHODOLOGY AND CHEMISTRY

As indicated in Figure 1, the lead **2** can be broken down conceptually into a BTZ core bearing three substituents (R1, R2, and R3). The structure−activity relationship (SAR) around groups R1 and R2 has been found to be very restrictive with little modification tolerated, while considerable variation in the structure of the R3 group is possible. In this study, the groups at R1 and R2 positions were fixed to NO_2 and CF_3, respectively, and only variations at position R3 were explored.

A BTZ specific ligand-based model was derived from 541 MIC values for 160 of the 170 compounds from the BTZ series[3] and 21 different bacterial organism/strains. The model was built using Bayesian statistics by correlating 2D molecular fingerprints of the compounds to their classification of being active (MIC < 1 μM) or inactive (MIC > 1 μM). For a compound predicted to be active, a predicted pMIC value was derived by interpolation from its nearest structural neighbor (most similar actives). Models were only derived for those

Received: June 29, 2012
Published: August 23, 2012

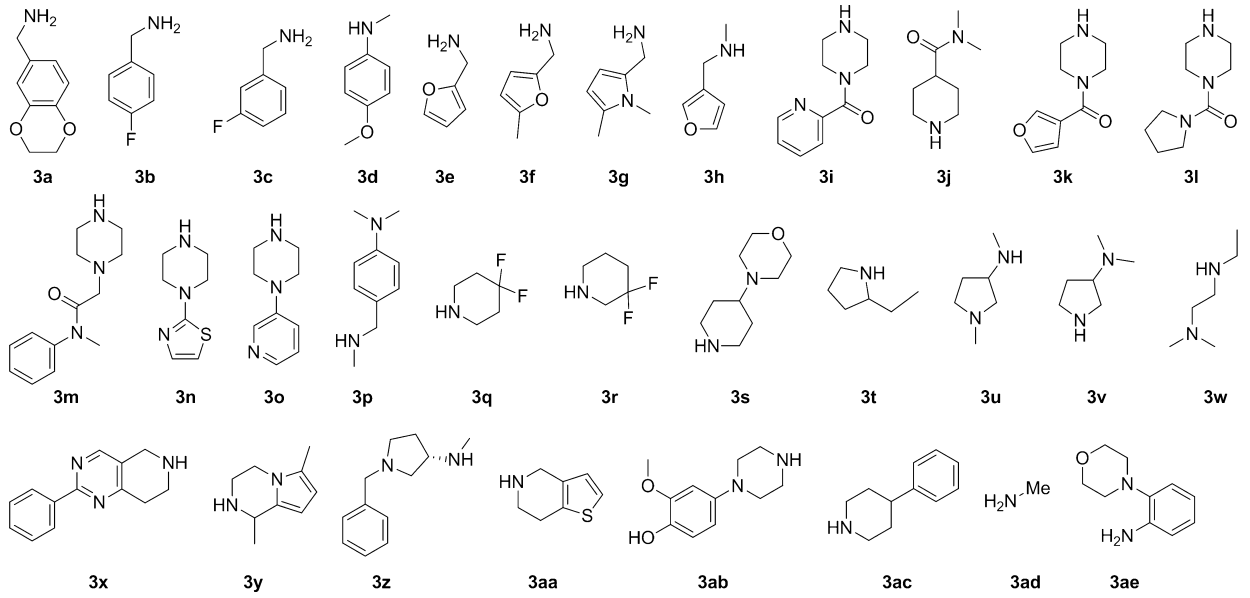

Figure 2. Amines selected by ligand-based design for exploration of the R3 position after addition to the BTZ core.

Scheme 1. Preparation of Spiroketal BTZ Derivatives[a]

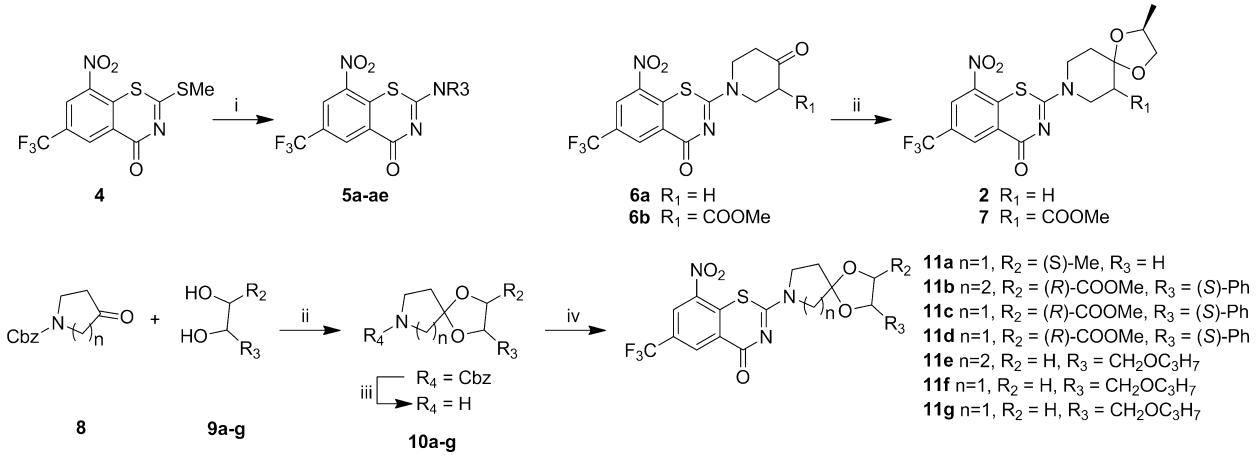

[a](i)EtOH, amines **3a**–**ae**, 60 °C; (ii) diol, DIPEA, TMSOTf, 0 °C, DCM, then ketone, TMSOTf, DCM, rt; (iii) 10% Pd/C, Et_3SiH or cyclohexene, MeOH; (iv) **4**, EtOH, 60 °C.

organism/strains having experimental MIC data for more than 20 compounds in the BTZ set, resulting in predictions for seven strains (Supporting Information Table S1). The predictability was then assessed by leave-one-out cross-validation. In all cases a good level of prediction was achieved. For example, for *Mtb* H37Rv, the model is able to correctly identify as actives 90% of the total number of truly active compounds, without including a single inactive compound in the prediction. For this model in particular, 60% of active compounds are assigned a predicted MIC within 10-fold of its corresponding experimental MIC. Poor aqueous solubility had been identified as a characteristic property of the BTZ series, and the most highly active compounds exhibit a low solubility. Therefore, predictive solubility models were included in the design of new compounds (Pipeline Pilot, Accelrys).[7]

On the basis of these models, a target list of novel BTZ analogues was generated to select a diverse set of R3 substituents with good predicted MIC and good predicted solubility. R3 amines from the 170 BTZ compounds were used as templates for virtual screening against the chemical catalogue containing 7.5 million commercial compounds, selecting structurally similar amines. After removal of molecules containing reactive groups, 2797 commercially available amines were selected. For each of the 2797 amines the corresponding BTZ compound was generated using virtual combinatorial chemistry. The resulting virtual compounds were filtered for molecular weight (350–500 Da), rotatable bonds (<8), and predicted solubility (log $S > -6.5$). Further filtering was carried out using the predictive MIC model for *Mtb* H37Rv, removing compounds that were either predicted to be inactive or outside the applicability domain of the model. The resulting 333 compounds were divided into 20 clusters using the FCFP_4 2D fingerprints and nearest-neighbor clustering. Within each cluster the three compounds with highest predicted solubility (log *S*) were selected.

From these compounds 28 amines (**3a**–**ab**) were selected based on availability and cost (Figure 2). A further 3 amines (**3ac**–**ae**) outside the predictive models were also chosen. The target compounds were prepared by nucleophilic addition of amines to thiomethyl benzothiazinone **4**[4,8] to give the BTZ

dx.doi.org/10.1021/jm3008882 | *J. Med. Chem.* 2012, 55, 7940–7944

Table 1. Antibacterial, Stability, and Toxicity Testing Data for Selected BTZ Compounds[a]

compd	MIC [μg/mL] *M. smeg*,[b] *M. fort.* B,[c] MDR-TB[d]	stability [%] buffer, plasma,[e] microsome[f]	toxicity [μM] HUVEC,[g] K-562,[g] HeLa[h]	compd	MIC [μg/mL] *M. smeg*,[b] *M. fort.* B,[c] MDR-TB[d]	stability [%] buffer, plasma,[e] microsome[f]	toxicity [μM] HUVEC,[g] K-562,[g] HeLa[h]
2	0.008	98	8	**5q**	0.25	101	ND[i]
	0.00156	107/97	11		>0.1	64/92	ND[i]
	≤0.015	98/45	>50		≤0.125	61/80	ND[i]
5a	0.004	91	20	**5z**	0.004	96	18
	0.012	86/114	37		ND[i]	92/114	30
	0.03	43/32	41		>0.03	6/7	38
5g	0.125	14	17	**5ac**	0.004	82	>50
	0.05	108/93	21		0.0125	96/71	>50
	≤0.125	28/37	48		≤0.015	120/75	>50
5m	0.015	78	18	**7**	0.015	98	16
	0.0125	95/115	30		0.0125	51/56	22
	0.03	13/2	39		>0.1	81/29	36
5n	0.25	98	ND[i]	**11b**	0.015	82	>50
	0.025	99/111	ND[i]		0.00625	90/88	>50
	≤0.125	42/13	ND[i]		>0.03	ND/ND[i]	>50
5p	0.001	95	>50	**11e**	0.004	99	>50
	0.00625	90/104	>50		0.0031	98/103	>50
	0.03	6/8	>50		≤0.015	6/9	43

[a]All compounds showed CC_{50} of >10 μM against HepG2 and HEK293 cell lines. [b]*M. smegmatis* 700084. [c]*M. fortuitum* B. [d]*M. tuberculosis* 2745/09 MDR. [e]Human/mouse. [f]Liver microsomes human/mouse. [g]GI_{50}. [h]CC_{50}. [i]Not determined.

analogues **5a**–**ae** (Scheme 1). This process allows for a very convenient point of convergence in the synthesis, as **4** can be prepared on large scale and nucleophilic amines can then be readily added into the R3 position. For analogues **5t**, **5x**, **5y**, and **5aa** insufficient quantities of the desired products were obtained for assay after several attempts at synthesis and the compounds were not pursued further for this study.

The methodology used to design **5a**–**ab** selects only amines that are commercially available. To explore the region around the spiroketal of **2**, an additional group of compounds was designed where chemical steps were required in preparation of the amines (Scheme 1). While formation of the ketals using standard Dean–Stark conditions was found to be tedious on small scale, a one pot version of the TMSOTf catalyzed addition of the bis-TMS ether of the diol[9] proved to be very rapid and yielded clean products. This procedure could be applied to ketones already installed on the BTZ core (e.g., **6a**, **6b**), or on a N-protected aminoketone (**10a**–**g**) before deprotection and condensation with **4**. For several of the spiroketal compounds, diastereomers were formed at the spiro junction. In most cases the diastereomers were not separable and the compounds were assayed as mixtures. However, for two compounds these diastereomers were separable by preparative HPLC and were assayed independently (**11c**/**11d** and **11f**/**11g**, respectively).

To compare the compounds in this study with the previous results, we tested each compound in MIC assays for *M. smegmatis* 700084 using two different media: Middlebrook 7H9 and Mueller–Hinton broth. Most of the compounds showed only slightly different MIC values, within a log difference in the two broths (Table S3). The only exception was **5ac**, which showed 3 orders of magnitude higher activity (lower MIC) when assayed in Mueller Hinton broth. This compound also exhibits very low aqueous solubility (around 60 nM), which may be responsible for the different MIC values. In general all the assays using the MHB as growth medium resulted in slightly lower MIC values (higher activity) compared to the assays using the 7H9. Active compounds were then tested for mammalian cell cytotoxicity against HepG2 and HEK293 cells.

By use of this initial testing data, the active compounds were subjected to further testing for MIC against *M. smegmatis* SG987, *M. vaccae* 10670, *M. fortuitum* B, *M. aurum* SB66, and MDR-TB 2745/09, stability in buffer and human and mouse liver microsomes, antiproliferative effects, and cytotoxicity (Tables 1 and S4).

DISCUSSION AND CONCLUSIONS

MIC testing revealed several compounds that were more active or equivalent to **2** against *M. smegmatis* (**5p**, **5m**, **5z**, **5ac**, **11b**, **11e**, and **7**) and MDR-TB (**5a**, **5p**, **5z**, **5ac**, **11b**, and **11e**). The observed therapeutic indices (CC_{50}/MIC) were excellent for candidate antimicrobials (>10 000), notably for **5p** (>50 000) and **5ac** (>12 500), for which the indices greatly exceeded that of compound **2** (>6250). The differences were more pronounced when comparing antiproliferative effects (GI_{50}/MIC of >50 000, >12 500, and 1190, respectively). The compounds were generally stable to buffer and human and mouse plasma and liver microsomes. However, reduced stability was observed for **5g**, **5n**, **5m**, **5p**, **5z**, and **11e**. With a view to future in vivo studies, it was interesting to note the difference in stability in the presence of human or mouse microsomes observed for some compounds (eg **2**, **5m**, **5n**, and **7**). Evidence that the newly designed compounds retain the mode of action of compound **2** was shown in the lack of activity against *M. aurum* SB66 as the orthologous enzyme possesses a serine rather than a cysteine at residue 387, known to be critical to the action of the BTZ class.[3]

Of the 24 compounds tested from the in silico design approach, 13 were found to have activities against *M. smegmatis* of better than 1 μg/mL, while only two compounds were found to be inactive at our highest test concentration (2 μg/mL), indicating about a 90% success rate for the model at predicting active compounds (Table S2). The kinetic solubility of a selected group of compounds was measured at pH 7.4 using the

methods described by Alsenz,[10] Hoelke,[11] and Lipinski.[12] For two compounds there was a large variation observed between the duplicate determinations and they could only be placed qualitatively in the partially soluble band.[13] As can be seen in Table 2, the predicted solubility values were found to be within a log unit of those measured experimentally. Four compounds had equivalent or improved solubility relative to **2**.

Table 2. Comparison of Predicted and Measured Solubility

		measured result	
compd	predicted log *S*	log *S*	μM
2	−4.73	−5.16	6.8
5e	−5.09	−5.79	1.63
5f	−5.31	−5.74	1.82
5h	−5.03	partially soluble	
5j	−4.83	partially soluble	
5k	−5.38	−4.66	21.8
5m	−5.85	−4.93	11.9
5q	−5.17	−5.09	8.1
5w	−4.94	−4.98	10.6
5z	−6.05	−5.53	2.97
5ac	−6.94	−7.23	0.060

To compare the newly designed compound in this study and the previous BTZ compound, a structure diversity analysis was performed. By use of 2D fingerprints (ECFP_6) and Tanimoto distances, a distance matrix between each of the original BTZs and our new compounds was calculated. For visual representation of the distances between each compound, standard multidimensional scaling (MDS) has been applied to reduce the multidimensional distance matrix to two dimensions (distances within the two-dimensional plot represent the structural distances in the matrix)

As Figure 3 illustrates, the compounds designed and synthesized in this study were within the same broad structure

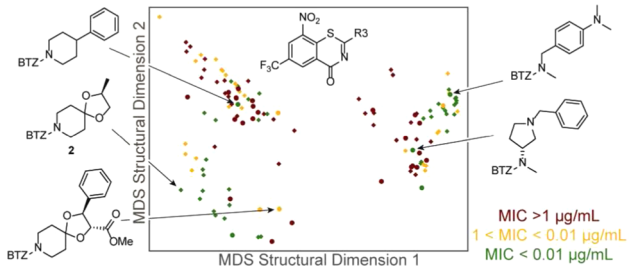

Figure 3. Multidimensional scaling (MDS) plot of the structural similarity/diversity of analogues of **2**, using 2D chemical fingerprints (ECFP_6) and Tanimoto distances to calculate the diversity between compounds. Original BTZ compounds are shown as diamonds and the newly designed compounds in this study as circles. The MIC activity is indicated by the color of the symbols, showing compounds with low MIC activity (MIC > 1 μg/mL) in dark red, medium MIC activity (1 < MIC < 0.01 μg/mL) in orange, and high MIC activity (MIC < 0.01 μg/mL) in green.

space as the original BTZ compounds. While the ligand-based in silico design is biased by the training set of BTZ compounds, the selection of compounds for synthesis was targeted for maximum structural diversity.

In the MDS plot the compounds fall into three structural clusters: (i) linear amines, (ii) cyclic amines (piperidines and piperazines), and (iii) the closely related piperidinespiroketals. Each group or area in the plot contains highly active compounds and low or inactive compounds, suggesting that the target does not have a single preferred structure for the R3 position and that it should be possible to tune compound pharmacokinetic properties by varying the R3 moiety. Indeed, highly active compounds have been found with solubilities ranging from 60 nM (**5ac**) to 12 μM (**5m**) and calculated log *P* values ranging over 3 orders of magnitude.

The ligand based modeling method used has shown a remarkable ability to distinguish actives from inactives for antitubercular BTZs and has allowed the exploration of the SAR within the broad structural space of the training set. The ability to bias the compound set toward any desired calculated physical property allows the refinement of the pharmacokinetic properties of the products. The extensive toxicity and stability data obtained allow us to select compound classes to progress into more detailed SAR studies and subsequent animal models.

■ ASSOCIATED CONTENT

Ⓢ Supporting Information

Details of synthesis and characterization, modeling, and biological assays (including the first round assays and the full MIC and toxicity panel of the second round). This material is available free of charge via the Internet at http://pubs.acs.org.

■ AUTHOR INFORMATION

Corresponding Author

*Phone: +61 7 3346 2044. Fax: +61 7 3346 2090. E-mail: m.cooper@uq.edu.au.

Notes

The authors declare no competing financial interest.

■ ACKNOWLEDGMENTS

We acknowledge the assistance of David Vidal and Jordi Mestres of Chemotargets and Albert Hinnen, Vadim Makarov, and Stuart Cole for helpful discussions. Funding was provided by the National Health and Medical Research Council (NHMRC) Australia Fellowship 511105.

■ ABBREVIATIONS USED

pMIC, $-\log_{10}$(MIC expressed as molarity)

■ REFERENCES

(1) WHO. Towards Universal Access To Diagnosis and Treatment of Multidrug-Resistant and Extensively Drug-Resistant Tuberculosis by 2015. http://www.who.int/tb/publications/2011/mdr_report_2011/en/index.html (accessed May 16, 2012).

(2) (a) Ma, Z.; Lienhardt, C.; McIlleron, H.; Nunn, A. J.; Wang, X. Global tuberculosis drug development pipeline: the need and the reality. *Lancet* **2010**, *375* (9731), 2100−2109. (b) Villemagne, B.; Crauste, C.; Flipo, M.; Baulard, A. R.; Déprez, B.; Willand, N. Tuberculosis: the drug development pipeline at a glance. *Eur. J. Med. Chem.* **2012**, *51*, 1−16.

(3) Makarov, V.; Manina, G.; Mikusova, K.; Mollmann, U.; Ryabova, O.; Saint-Joanis, B.; Dhar, N.; Pasca, M. R.; Buroni, S.; Lucarelli, A. P.; Milano, A.; De Rossi, E.; Belanova, M.; Bobovska, A.; Dianiskova, P.; Kordulakova, J.; Sala, C.; Fullam, E.; Schneider, P.; McKinney, J. D.; Brodin, P.; Christophe, T.; Waddell, S.; Butcher, P.; Albrethsen, J.; Rosenkrands, I.; Brosch, R.; Nandi, V.; Bharath, S.; Gaonkar, S.; Shandil, R. K.; Balasubramanian, V.; Balganesh, T.; Tyagi, S.; Grosset, J.; Riccardi, G.; Cole, S. T. Benzothiazinones kill *Mycobacterium tuberculosis* by blocking arabinan synthesis. *Science* **2009**, *324* (5928), 801−804.

(4) Makarov, A. V.; Cole, S. T.; Mollmann, U. Benzothiazinone Derivatives and Their Use as Antibacterial Agents. U.S. Patent Appl. US 2009/0239851 A1, 2009.
(5) (a) Mikusova, K.; Huang, H.; Yagi, T.; Holsters, M.; Vereecke, D.; D'Haeze, W.; Scherman, M. S.; Brennan, P. J.; McNeil, M. R.; Crick, D. C. Decaprenylphosphoryl arabinofuranose, the donor of the D-arabinofuranosyl residues of mycobacterial arabinan, is formed via a two-step epimerization of decaprenylphosphoryl ribose. *J. Bacteriol.* **2005**, *187* (23), 8020−8025. (b) Wolucka, B. A. Biosynthesis of D-arabinose in mycobacteria—a novel bacterial pathway with implications for antimycobacterial therapy. *FEBS J.* **2008**, *275* (11), 2691−2711.
(6) (a) de Jesus Lopes Ribeiro, A. L.; Degiacomi, G.; Ewann, F.; Buroni, S.; Incandela, M. L.; Chiarelli, L. R.; Mori, G.; Kim, J.; Contreras-Dominguez, M.; Park, Y.-S.; Han, S.-J.; Brodin, P.; Valentini, G.; Rizzi, M.; Riccardi, G.; Pasca, M. R. Analogous mechanisms of resistance to benzothiazinones and dinitrobenzamides in *Mycobacterium smegmatis*. *PLoS One* **2011**, *6* (11), e26675. (b) Trefzer, C.; Rengifo-Gonzalez, M.; Hinner, M. J.; Schneider, P.; Makarov, V.; Cole, S. T.; Johnsson, K. Benzothiazinones: prodrugs that covalently modify the decaprenylphosphoryl-beta-D-ribose 2′-epimerase DprE1 of *Mycobacterium tuberculosis*. *J. Am. Chem. Soc.* **2010**, *132* (39), 13663−13665.
(7) Tetko, I. V.; Tanchuk, V. Y.; Kasheva, T. N.; Villa, A. E. P. Estimation of aqueous solubility of chemical compounds using E-state indices. *J. Chem. Inf. Comput. Sci.* **2001**, *41* (6), 1488−1493.
(8) Makarov, V. A. Process for the Preparation of 2-Amino-Substituted 1,3-Benzothiazine-4-ones. WO 2011/132070 A1, 2011.
(9) Tsunoda, T.; Suzuki, M.; Noyori, R. A facile procedure for acetalization under aprotic conditions. *Tetrahedron Lett.* **1980**, *21* (14), 1357−1358.
(10) Alsenz, J.; Kansy, M. High throughput solubility measurement in drug discovery and development. *Adv. Drug Delivery Rev.* **2007**, *59* (7), 546−567.
(11) Hoelke, B.; Gieringer, S.; Arlt, M.; Saal, C. Comparison of nephelometric, UV-spectroscopic, and HPLC methods for high-throughput determination of aqueous drug solubility in microtiter plates. *Anal. Chem.* **2009**, *81* (8), 3165−3172.
(12) Lipinski, C. A.; Lombardo, F.; Dominy, B. W.; Feeney, P. J. Experimental and computational approaches to estimate solubility and permeability in drug discovery and development settings. *Adv. Drug Delivery Rev.* **1997**, *23* (1−3), 3−25.
(13) Bevan, C. D.; Lloyd, R. S. A high-throughput screening method for the determination of aqueous drug solubility using laser nephelometry in microtiter plates. *Anal. Chem.* **2000**, *72* (8), 1781−1787.